Mesoscopic multiclass traffic flow modeling on multi-lane sections

Guillaume Costeseque, Aurélien Duret

Mesoscopic multiclass traffic flow modeling on multi-lane sections

Guillaume Costeseque*
Inria Sophia Antipolis - Méditerranée,
F-06902, Sophia Antipolis Cedex,
phone: +33 (0) 492 387 625,
guillaume.costeseque@inria.fr

Aurélien Duret
University of Lyon, F-69000, Lyon, France
IFSTTAR, LICIT, F-69500, Bron,
ENTPE, LICIT, F-69518, Vaulx en Velin,
phone: +33 (0) 472 142 331,
aurelien.duret@ifsttar.fr

Paper submitted for presentation to
Transportation Research Board 95th Annual Meeting
November 14, 2015

$4,940$ words + 7 figures + 1 table $\Rightarrow 6,940$ 'words'

Paper revised from original submission

*Corresponding author

Abstract

The aim of this paper is to propose a new event-based mesoscopic approach to model multi-class traffic flow on multi-lane road sections. The mesoscopic model was first proposed by Leclercq and Bécarie (2012) and turns out to be equivalent to the resolution of the seminal LWR model in Lagrangian-space coordinates $n - x$. It is fully consistent at a macroscopic scale with the LWR model while keeping track of individual vehicles. This is the reason why we talk about *mesoscopic* modeling since it combines both macroscopic and microscopic representations of traffic. It is not related to gas-kinetic models. Our model is built on Hamilton-Jacobi equations which have been proven to provide an efficient framework in traffic flow modeling for exact numerical methods at a low computational cost. The paper revisits the multi-class problem with a continuous moving bottleneck approach (instead of a sequential one), introducing a totally new capacity drop parameter for multi-lane sections. This capacity drop parameter, together with our multi-class modeling also overhauls the Daganzo diverge model with a relaxed FIFO assumption.

Keywords: mesoscopic; multiclass; multilane; Hamilton-Jacobi; FIFO; diverge.

Table of symbols

Symbol	Meaning
x	spatial location
t	time
n	vehicle label, Lagrangian coordinate
q	flow
k	density
v	speed
κ	maximal density for one lane
C	maximal flow for one lane
$-w$	wave speed (with $w > 0$)
u	free flow velocity
$k \mapsto Q(k)$	flow-density fundamental diagram
$r \mapsto H(r)$	headway-pace fundamental diagram
$h \ \left(= \frac{1}{q}\right)$	headway
$r \ \left(= \frac{1}{v}\right)$	pace
$s \ \left(= \frac{1}{k}\right)$	spacing
v_B	speed of the moving bottleneck
h_B	residual capacity up to the moving bottleneck
δ	capacity drop parameter
N	number of lanes
I	vehicle class

TABLE 1 Table of symbols used along the paper.

1 Introduction

Motivation and quick literature review

Dynamic traffic flow models are an essential building block for many applications including traffic flow monitoring, estimation and control. Previous works have already shown that simulation of traffic flow on a large scale network thanks to such dynamic models can be cumbersome, despite a lot of research effort made in that direction in the past decades. Classical dynamic models embed *microscopic* and *macroscopic models*. Microscopic traffic models allow a detailed representation of traffic thanks to an individual tracking of vehicles but at a high computational cost and with obvious calibration difficulties, depending on the number of vehicles that are simulated. Macroscopic models and in particular the celebrated first order LWR model [*1, 2*] provide a robust and easy way to compute traffic flow on networks but they generally fail to recapture some meaningful phenomenon like for instance the capacity drop, the bounded acceleration of vehicles or the stop-and-go waves, without being specifically adapted. For a review of microscopic and macroscopic traffic models, the interested reader is referred to [*3*]. One interesting microscopic car-following model for us is Newell's one [*4*].

As underlined in [*5*], there exists a third class of traffic flow models that are well adapted for network applications. These models are called *mesoscopic* because while being consistent with macroscopic traffic flow rules, they also allow a vehicular description, say a microscopic description. The mesoscopic version of the LWR model can be also interpreted into the Hamilton-Jacobi (HJ) framework as it was first properly established in [*6*]. See also references therein about the three dimensions representation of traffic (Eulerian for $t - x$ framework, Lagrangian for $t - n$ one and Lagrangian-space for $n - x$ one) and the variational techniques that can be used to solve such models.

To enrich the representation of macroscopic models, which basically use a one-lane aggregation, it is necessary, for real-world applications, to consider the variety of road users and of their behaviors. Some efforts have been made in that direction since the beginning of the 2000's by introducing *multiclass and multilane* (MCML for short) features into classical models such as kinetic ones [*7*] or as the seminal LWR model in Eulerian [*8*] or Lagrangian coordinates [*9*]. For an accurate overview of these MCML models, the reader is referred to [*9, 10*].

Another strategy to take into account the MCML features is to generalize the *moving bottleneck* (MB) problem for which the users are classically divided into a fast class, say the "rabbits", and a slower one, called the "slugs" (see [*11*] for the origin of these terms). The MB theory is now well structured since the pioneering works [*12, 13*]. See for instance [*6*] for one description of the MB problem in both mesoscopic and HJ framework.

The aim of this paper is precisely to revisit the MCML problem on a network by gathering the main advantages of all the techniques that have been developed separately up to now. As an application, we are concerned with a diverge for which we introduced a relaxation parameter of the First-In-First-Out (FIFO) rule which is in some cases violated or not really realistic as pointed out in the literature [*14, 15*] but which is still widely assumed in traffic engineering works for the sake of simplicity. Our guiding example is a diverge whenever at most one exit branch is congested.

Organization of the paper

The remaining of the paper is structured as follows: in Section 2, some basic theoretical elements which serve us as building blocks for our model, are recalled. Then in Section 3, the new MLMC model is introduced and the adapted numerical scheme is presented in Section 4. In Section 5, some numerical examples are provided. Finally, in Section 6, the main results are wrapped up and some future directions of research are pointed out.

2 Recap of some useful concepts

2.1 Mesoscopic modeling

The mesoscopic resolution of the well-known LWR model proposed in [5] allows to compute the passing times of vehicles at a certain number of specific points of the network (the intersections for instance): it is thus called an event-based model keeping track of vehicles. The name "mesoscopic" came from the fact that the approach combines vehicular description with macroscopic behavioral rules. It is noteworthy that this is not related to gas-kinetic models. This $n - x$ representation is fully consistent with the macroscopic (Eulerian) framework, say the original LWR model, and with the microscopic (Lagrangian) framework, say microscopic car-following models. The mesoscopic resolution is able to track vehicles on the network, which is an advantage compared to previous Eulerian approach resolution (for instance for network application). The mesoscopic resolution presents a calculation time that only depends on the number of events during the simulation which is again an advantage compared to the previous microscopic resolution for which the calculation time increases when the network is congested.

Following [6], let us introduce the headway h (time gap between two successive vehicles), the pace r (travel time per space unit) and the spacing s (spatial gap between two successive vehicles). One has the following relations

$$q = \frac{1}{h}, \quad v = \frac{1}{r}, \quad k = \frac{1}{s}, \quad q = kv, \quad \text{and} \quad h = rs$$

where q, v and k denote respectively the flow, the speed and the density.

We now define the Lagrangian variable as

$$n = N(t, x) := \int_x^\infty k(t, \xi) d\xi$$

where $N(t, x)$ gives us the label of the vehicle located at position x at time t. We are now ready to introduce $T(n, x)$ the passing time of vehicle n at location x as follows

$$T(n, x) := \int_x^\infty r(n, \xi) d\xi.$$

One can verify that

$$\begin{cases} \partial_t N = q, & \text{(flow)} \\ \partial_x N = -k, & \text{(density)} \end{cases}, \quad \text{and} \quad \begin{cases} \partial_n T = h, & \text{(headway)} \\ \partial_x T = r, & \text{(pace)} \end{cases}$$

We recall that the first order LWR model [1, 2] is given by the following scalar conservation law

$$\partial_t k + \partial_x Q(k) = 0 \tag{1}$$

with $k(t,x)$ the density and $Q : \mathbb{R} \to \mathbb{R}$ the flow-density Fundamental Diagram (FD). One has

$$Q\left(k(t,x)\right) := k(t,x)V\left(k(t,x)\right)$$

where $V : \mathbb{R} \to \mathbb{R}$ denotes the speed-spacing FD.

Applying the above change of coordinates, (1) becomes in Lagrangian-space framework

$$\partial_n r - \partial_x h = 0 \tag{2}$$

where we assume that the headway is a function of the pace $h = H(r)$.

The *variational* theory, say the Hamilton-Jacobi (HJ) formulation of the conservation law (2), teaches us that if $r = \partial_x T$ solves (2), then T satisfies the following Hamilton-Jacobi equation

$$\partial_n T - H\left(\partial_x T\right) = 0, \quad \text{for} \quad (n,x) \in [0,+\infty) \times [0,+\infty). \tag{3}$$

Consider the following boundary conditions

$$\begin{cases} T(n,0) = \check{g}(n), & \text{for any} \quad n \in [0,+\infty), \\ T(0,x) = G(x), & \text{for any} \quad x \in [0,+\infty). \end{cases} \tag{4}$$

For sake of simplicity, assume here that we consider a one-lane section ($N = 1$). If moreover we consider a triangular Fundamental Diagram (also called Hamiltonian) H,

$$H(r) = \begin{cases} \dfrac{1}{\kappa} r + \dfrac{1}{w\kappa}, & \text{if} \quad r \geq \dfrac{1}{u}, \\ +\infty, & \text{otherwise}, \end{cases} \tag{5}$$

then the representation formula known as the Lax-Hopf formula, for the associated HJ equation (3)-(4) for which $T(n,0)$ for any n (passing times of all vehicles at upstream position) and $T(0,x)$ for any x (passing times of the first vehicle) are known and piecewise constant,

$$T(n,x) = \sup_{\left\{(n_0,x_0,X(\cdot)) \text{ s.t. } \middle| \begin{smallmatrix} X(n_0)=x_0, \\ X(n)=x \end{smallmatrix}\right\}} \left\{ T(n_0,x_0) + \int_{n_0}^{n} H^{\boxtimes}\left(-\dot{X}(\xi)\right) d\xi \right\},$$

simply boils down to a maximization problem between two terms (see [6]):

$$T(n,x) = \max\left\{ T(n,0) + \frac{x}{u},\ T(0,x+n\sigma) + n\tau \right\}, \tag{6}$$

with u denotes the free flow speed, $\sigma := \dfrac{1}{\kappa}$ the jam spacing (or minimal spacing) and $\tau := \dfrac{1}{w\kappa}$ the wave trip time between two consecutive vehicles in congestion (recall that $w > 0$). Indeed, the *concave Fenchel transform* $H^{\boxtimes}$ of H is given by

$$H^{\boxtimes}(s) := \inf_{p \in \mathrm{Dom}(H)} \{H(p) - ps\}$$

and if H is given by (5), then it follows

$$H^{\boxtimes}(s) = \begin{cases} \dfrac{1}{\kappa}\left(\dfrac{1}{u} - \dfrac{1}{w}\right) - \dfrac{s}{u}, & \text{if} \quad s \geq \dfrac{1}{\kappa}, \\ -\infty, & \text{otherwise.} \end{cases}$$

See also [16] for explicit (generalized) Lax-Hopf formula to compute the solution of (3) with the assumption of a piecewise affine Hamiltonian and under piecewise affine internal boundary conditions.

2.2 Moving bottleneck theory

Following [6, 12, 13], a *moving bottleneck* is defined as a vehicle (or a platoon of vehicles) defining by itself a class of vehicles, for instance trucks or buses, which has a maximal free flow speed which is lower than the free flow speed of its immediate following vehicle (or immediate following platoon of vehicles).

A moving bottleneck is said to be *active* if and only if it generates queues at upstream positions with respect to the moving bottleneck and if the upstream state is different from the downstream state.

We just recall the notations and the main steps for the computation of the *passing rate* (say the flow that can overtake the moving bottleneck) in the Eulerian framework (see Figure 1). Let us denote by:

- $\xi_N(t)$ the trajectory of the moving bottleneck in time-space plane $t - x$,
- $\xi_T(n)$ the location where the vehicle n crosses the bottleneck in Lagrangian-space plane $n - x$,
- $v_B(t) := \dot{\xi}_N(t)$ the moving bottleneck speed which is upper bounded by v_b,
- $k_D := k\left(t, \xi_N(t)^+\right)$ the density downstream of the bottleneck,
- $q_D := Q(k_D)$ the flow downstream of the bottleneck,
- $R(v_B, q_D)$ the maximum bottleneck passing rate

$$R(v_B, q_D) := q_D - k_D v_B.$$

Notice that

$$\dot{\xi}_T(n) = \frac{v_B}{R(v_B, q_D)}.$$

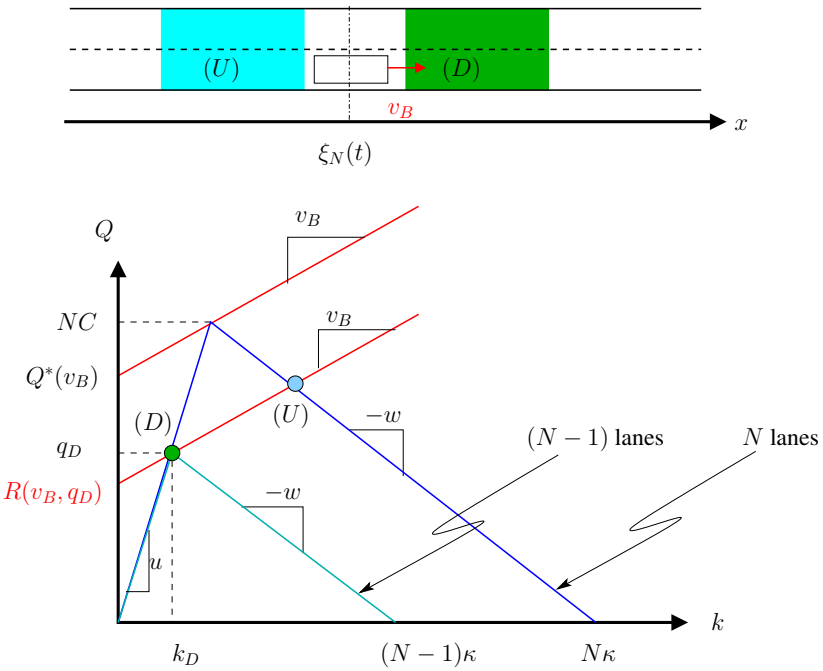

FIGURE 1 Moving bottleneck graphical solution in Eulerian coordinates, for a triangular Hamiltonian or flow-density FD defined as $Q(k) = \min\{uk, w(\kappa - k)\}$, with k the density. (U) and (D) denote respectively the upstream and downstream traffic state with respect to the moving bottleneck position.

In Eulerian framework, the mathematical problem reads as a coupled ODE-PDE problem for which existence result holds (but uniqueness is still an open problem) [17]

$$\begin{cases} \partial_t k + \partial_x \left(Q(k)\right) = 0, & \text{for any} \quad t > 0, \quad x \in \mathbb{R}, \\ Q(k(t, \xi_N(t))) - \dot{\xi}_N(t) k(t, \xi_N(t)) \leq \alpha Q^* \left(\dot{\xi}_N(t)\right), & \text{for any} \quad t > 0, \\ \dot{\xi}_N(t) = \min\left\{v_b,\ V\left(k(t, \xi_N(t)^+)\right)\right\}, & \text{for any} \quad t > 0, \end{cases} \tag{7}$$

together with the following initial conditions

$$\begin{cases} k(0, x) = k_0(x), & \text{on} \quad \mathbb{R}, \\ \xi_N(0) = \xi_0. \end{cases} \tag{8}$$

In (7), the PDE leads the evolution of the density of vehicles while the ODE gives us the trajectory of the moving bottleneck. The coupling condition is the constraint imposed by the moving bottleneck on the traffic flow. For a complete presentation of the model in Eulerian coordinates, the reader is referred to [17] and references therein.

The coefficient $\alpha \in]0, 1[$ in (7) gives the reduction rate of the road capacity due to the presence of the moving bottleneck. It is indeed the ratio of available lanes for the overtaking maneuvers. If N denotes the number of lanes on the road section and if the moving bottleneck is located on the

rightmost lane, then

$$\alpha = \frac{N-1}{N}.$$

The upper bound on the passing rate in (7) is defined as a function of the moving bottleneck speed $v_B(t) \mapsto Q^*(v_B(t))$ and it matches the *Legendre-Fenchel transform* of the flow-density FD Q (for the N lanes)

$$Q^*(v) := \sup_{\rho \in \mathrm{Dom}(Q)} \{Q(\rho) - v\rho\}.$$

The Eulerian model (7) can be easily extended to the Lagrangian-space framework. It will be presented in the next section for our MCML application. The full solution details for the mesoscopic LWR model are given in Section 5.2 of [6]. However, it is noteworthy that in any case (say if the vehicle is constrained by the downstream traffic conditions –the moving bottleneck is inactive– or if the vehicle is constrained by the moving bottleneck –the moving bottleneck is active–), the passing time of a vehicle n at position x of the network is determined as the maximum between the passing time of vehicle n at upstream position $(x - \Delta x)$ plus the travel time obtained at free flow speed on the section $[x - \Delta x, x]$ (or eventually reduced due to the active moving bottleneck) and the passing time of the leader vehicle $(n-1)$ at downstream position $(x + \Delta x)$ translated by the jam speed.

It is worth noticing that all the material of this Section 2 is extracted from existing works. These results will served as the fundamental background for our building blocks that are presented in next Section 3.

3 Mesoscopic formulation of multiclass multilane models

3.1 Choice of the modeling

For tackling the multi-class and multi-lane modeling (whatever the network is), we can consider:

- either generic multi-class models (see for instance [10]) that classically fall into the Generic Second Order Model (GSOM) family [18] with a class-dependent fundamental diagram. In this case, on can define the vehicular attribute as the class of the considered vehicle.
- or the moving bottleneck theory thanks through a coupled system of conservation laws (or equivalently of Hamilton-Jacobi equations) extending what was previously done in the literature (see for instance [17]).

In the first case, we cannot use the strength of the mesoscopic formulation since we have to define the indices of the vehicles, once and for all, and it is not straightforward to deal with the re-labeling of the vehicles once we consider overtaking maneuvers between each class.

In the second case, each class has its own labeling and by assuming that inside a class the vehicles respect the FIFO rule, they stay ordered at any time. Apart from this fundamental difference,

both approaches are quite close since we consider a fundamental diagram (or Hamiltonian) which depends on an "attribute" denoted by I and defined as the vehicle class and the lane (which is the case in the remaining of the paper) or the Origin-Destination pattern or a combination of both.

3.2 Modeling assumptions

Consider a stretch of road $[x_0, x_1]$ composed by N separate lanes with traffic stream composed of fast and slow vehicles defining two classes of users called respectively "rabbits" ($I = I_1 = 1$) and "slugs" ($I = I_2 = 2$). In all that follows, notice that we will use indifferently the terms rabbits or fast vehicles and slugs or slow vehicles.

It is assumed that one vehicle cannot belong simultaneously to more than one class but its class can evolve with respect to time (according to the traffic state or to the mental stress of the driver or to its path on the network for instance). In the remaining, the class attribute is assumed to not depend on time.

Slugs cannot go to the passing lane(s) and are limited to the shoulder lane, while the fastest vehicles can use the passing lane(s) and the shoulder lane.

Let us introduce the class-dependent headway-pace FD (or Hamiltonian)

$$H : (r, I) \mapsto H(r, I)$$

for a given class attribute $I \in \{1, 2\}$.

(A0) We assume that $r \mapsto H(r, \cdot)$ is convex.

3.3 Capacity drop parameter

One of the main drawback of the LWR model (whatever the chosen resolution is) is that the capacity drop phenomenon is not represented. *Capacity drop* can be characterized as a reduction in discharge flow after queue formation that is observed at the downstream of an active (moving) bottleneck location. Basically this difference of flow is interpreted as a recovery flow from low speeds (vehicles stuck in a congestion) to free flow (vehicles accelerating). Below, we describe a strategy to take into account this well-known feature of traffic flows.

3.3.1 Capacity drop and moving bottleneck

Consider a parameter $\delta \in [0, 1]$ that tells us how much the traffic flow complies to the First-In-First-Out (FIFO) rule, with the two extreme cases:

- If $\delta = 0$, the traffic is strictly non-FIFO, say all the vehicles can overtake each other without any restriction, say they can use the entire residual headway h_B of the passing lane(s).

- If $\delta = 1$, the traffic is strictly FIFO, say the vehicles keep ordered at all time, independently of their origin and/or destination and even if there are some available passing lane(s). The vehicles behave as if the residual headway is equal to zero.

An intermediate value $\delta \in]0,1[$ can be interpreted as a penalty for overtaking maneuvers by reducing the residual headway of the passing lane(s) (say the available headway for vehicles arriving on the closest moving bottleneck and that want to overtake it) to a modified residual headway (say the real available headway for vehicles that are going to overtake)

$$\tilde{h}_B := \frac{1}{1-\delta} h_B.$$

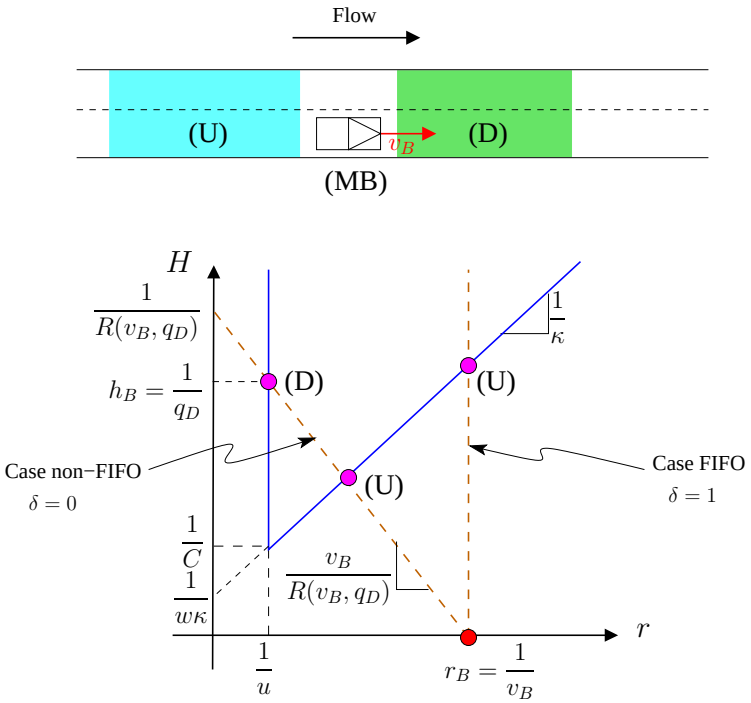

FIGURE 2 Moving bottleneck graphical solution in Lagrangian-space coordinates, for a triangular Hamiltonian or headway-pace FD $H(r)$ defined in (5) with r the pace, and for different values of the capacity drop parameter δ. (U) and (D) denote respectively the upstream and downstream traffic state with respect to the moving bottleneck position.

In Figure 2, one can notice that with a strict non-FIFO behavior, whenever the moving bottleneck is active, the upstream traffic state is different from the downstream traffic state. Conversely, if one assumes a strict FIFO behavior, all the vehicles upstream have to adopt the moving bottleneck speed v_B.

Interestingly, our approach finds a different application in a work by Laval [*19*] that deals with the modeling of two-lane rural roads. In this framework, the opposite traffic flow acts as a reduction of the ability of vehicles to overtake a moving bottleneck. This is very similar to our capacity drop parameter δ. Still in [*19*], Laval gives the analytical expression of the travel time as a function of the proportion of slow vehicles.

3.3.2 Relaxing the FIFO assumption at a diverge

The parameter δ introduced in the previous subsection for road sections, can be extended to spatial discontinuities of the network. In this paper, we are particularly concerned with diverges. In such a case, introducing the parameter δ is equivalent to relax the FIFO assumption.

Let us consider a diverge composed of one incoming road that divides into J outgoing branches (with $J \geq 2$). The original model of Daganzo [20] (equivalent to the first diverge model used in [21] and also to the one in [22], see [23] for a detailed review of the literature on diverge models) relies on the FIFO assumption that is reasonable for the following traffic cases:

- the traffic state is in free flow condition on all downstream branches,
- the traffic state is congested on all downstream branches.

Nonetheless, as soon as at least one downstream branch is in free flow condition while another downstream branch is congested, the FIFO assumption is no longer realistic.

The idea is then to introduce a relaxation parameter $\delta \in [0, 1]$ that represents the percentage of vehicles that can go through the diverge in direction of the exiting branch, even if the node is congested. This parameter is exactly the same than the capacity drop parameter introduced in the previous section. In the case of a diverge, this parameter allows us to relax the FIFO assumption upstream to the diverge.

Let us denote by

- Δ_0, the upstream demand,
- Δ_j, the proportion of the demand that wants to exit on downstream branch j,

$$\Delta_j := \gamma_j \, \Delta_0, \quad \text{for any} \quad j,$$

- Σ_j, the downstream supply on branch j,
- C_j, the capacity of branch j, say the maximal flux that can be passed on the road,
- γ_j, the proportion of the flow that goes in direction of branch j. Note that one has $\sum_j \gamma_j = 1$ and without loss of generality, we assume that $\gamma_j > 0$ for any j.
- q_0, the flow on the unique upstream branch and q_j the flow on downstream branch j. We have that for any j

$$\begin{cases} q_j = \gamma_j \, q_0, & \text{(Flow distribution)} \\ \\ q_j \leq \Sigma_j \leq C_j, & \text{(Supply constraint)} \end{cases}$$

There are several cases to distinguish:

1. If no upstream demand exceeds its downstream supply, say $\Delta_j \leq \Sigma_j$ for any j or equivalently $\Delta_0 \leq \min\limits_j \left\{ \dfrac{\Sigma_j}{\gamma_j} \right\}$, then the solution is provided by the classical Daganzo model

$$\begin{cases} q_0 = \Delta_0, \\ q_j = \Delta_j = \gamma_j \Delta_0 = \gamma_j \, q_0, \qquad \text{for any} \quad j. \end{cases}$$

2. If all upstream demands exceed the downstream supplies, say $\Delta_j > \Sigma_j$ for any j or equivalently $\Delta_0 > \max\limits_j \left\{ \dfrac{\Sigma_j}{\gamma_j} \right\}$, then the solution is (also) provided by the classical Daganzo model

$$\begin{cases} q_0 = \displaystyle\sum_j \Sigma_j < \sum_j \Delta_j = \Delta_0, \\ q_j = \Sigma_j < \Delta_j, \qquad\qquad\qquad \text{for any} \quad j. \end{cases}$$

3. If at least one upstream demand exceeds its downstream supply, but one of the downstream branch is in free flow condition, say $\min\limits_j \left\{ \dfrac{\Sigma_j}{\gamma_j} \right\} < \Delta_0 < \max\limits_j \left\{ \dfrac{\Sigma_j}{\gamma_j} \right\}$, we denote by J^* the set of all downstream branches that are in free flow condition and we set

$$\bar{q} := \min_k \left\{ \frac{\Sigma_k}{\gamma_k} \right\}.$$

Then the solution is provided by the modified model (with the parameter $\delta \in [0,1]$)

$$\begin{cases} q_0 = \delta \bar{q} + (1-\delta) \left[\displaystyle\sum_{j \notin J^*} \Sigma_j + \sum_{j \in J^*} \Delta_j \right], \\ q_j = \delta \gamma_j \bar{q} + (1-\delta) \Sigma_j, \qquad\qquad \text{for any} \quad j \notin J^*, \\ q_j = \delta \gamma_j \bar{q} + (1-\delta) \Delta_j, \qquad\qquad \text{for any} \quad j \in J^*. \end{cases}$$

For a full-non FIFO model ($\delta = 0$), we get

$$\begin{cases} q_0 = \displaystyle\sum_{j \notin J^*} \Sigma_j + \sum_{j \in J^*} \Delta_j < \sum_j \Delta_j = \Delta_0, \\ q_j = \Sigma_j, \qquad\qquad\qquad\qquad \text{for any} \quad j \notin J^*, \\ q_j = \Delta_j, \qquad\qquad\qquad\qquad \text{for any} \quad j \in J^*, \end{cases}$$

while taking $\delta = 1$ gives us the classical FIFO model

$$\begin{cases} q_0 = \bar{q} < \displaystyle\sum_j \Delta_j = \Delta_0, \\ q_j = \gamma_j \bar{q} < \Delta_j, \quad \text{for any} \quad j. \end{cases}$$

All the details are given for flows for the reader convenience because that the Eulerian framework is the most well-known in the community up to now. However, notice that all the approach can be conversed to headway without any difficulty.

3.4 Expression of the MCML model

In this subsection, we finally summarize the previous contributions (old –Section 2– and new –Section 3–) into a unique multiclass and multilane mesoscopic model, expressed in Lagrangian-space coordinates.

Assume that each class satisfies to a LWR model with a specific fundamental diagram that depends on the attribute I. Consider two headway-pace fundamental diagrams $H(\cdot, I_1)$ and $H(\cdot, I_2)$. We assume that the vehicles belonging to class 1 are faster than the ones of class 2. Thus, one has $u_1 > u_2$ (where we recall that u_i is the top speed of class i). In the discrete application presented in next Section, we consider that H are piecewise linear. See (11) for an example of the chosen Hamiltonians. In that setting, the maximal speeds of each class are different but the congestion wave and the jam density are conserved.

Moreover, we define the concave Legendre-Fenchel transform of the class-specific Hamiltonian $H(\cdot,\cdot)$ with respect to its first variable, as follows

$$H^{\boxtimes}(s, I) := \inf_{r \in \mathrm{Dom}(H(\cdot, I))} \{H(r, I) - sr\}, \quad \text{for any} \quad (s, I) \in \mathbb{R} \times \mathbb{R}.$$

Let $(n_0, x_0, x_1) \in \mathbb{R}^3$ be fixed such that $x_0 < x_1$. The complete model in HJ framework writes as a system of coupled PDEs

$$\begin{cases} \partial_n T_1 - H\left(\partial_x T_1, I_1\right) = 0, & \text{for} \quad (n,x) \in [n_0, +\infty) \times [x_0, x_1], \\ \partial_n T_2 - H\left(\partial_x T_2, I_2\right) = 0, & \text{for} \quad (n,x) \in [n_0, +\infty) \times [x_0, x_1], \\ H\left(\partial_x T_1(n, \xi(n)), I_1\right) - (1-\delta)\dot{\xi}\left(n_2^*\right) \partial_x T_1(n, \xi(n)) & \\ \qquad \geq \dfrac{1}{\alpha} H^{\boxtimes}\left((1-\delta)\dot{\xi}\left(n_2^*\right), I_1\right) & \text{for} \quad n \in [n_0, +\infty), \\ T_2\left(n, \xi(n)\right) \geq T_1(n_1^*, \xi(n)) + H\left(\partial_x T_1(n_1^*, \xi(n)), I_2\right), & \text{for} \quad n \in [n_0, +\infty), \end{cases} \tag{9}$$

where

$$\begin{cases} n_2^* := \text{argmax } T_2(\cdot, \xi(n)) \quad \text{and} \quad \xi(n) = \xi(n_2^*), & \text{for} \quad n \in [n_0, +\infty), \\ n_1^* := \text{argmax } T_1(\cdot, \xi(n)) & \text{for} \quad n \in [n_0, +\infty), \end{cases}$$

and with the following mixed Neumann-Dirichlet boundary conditions

$$\begin{cases} \partial_n T_i(n, x_0) = \check{g}_i(n), & \text{on} \quad [n_0, +\infty), \\ \partial_n T_i(n, x_1) = \hat{g}_i(n), & \text{on} \quad [n_0, +\infty), \quad \text{for} \quad i \in \{1, 2\}. \\ T_i(n_0, x) = G_i(x), & \text{on} \quad [x_0, x_1], \end{cases} \tag{10}$$

(A1) Assume that $\check{g}_i$, $\hat{g}_i \in C^0(\mathbb{R})$ and $G_i \in C^1(\mathbb{R})$.

In (9), the first two equations express the conservation of vehicles in Lagrangian-space coordinates and inside each vehicle class (independently of the other one).

Assume that n_i^* ($i \in \{1, 2\}$) denotes the nearest leader from class i for vehicle n of class $j \neq i$ ($j \in \{1, 2\}$). It is computed as the last vehicle that has passed through the current location of vehicle n.

The third equation is the coupling condition from the point of view of class 1, say the moving bottleneck condition whenever a vehicle of class 1 catches a slower vehicle of class 2, whose label is assumed to be n_2^*. This inequality gives a lower bound on the *modified* passing headway. Due to the capacity drop parameter $\delta \in [0,1[$ (which also stands for the relaxation of the FIFO assumption on a diverge), the modified passing headway $\tilde{H}$ is determined as follows

$$\tilde{H} = \frac{1}{1-\delta} h_B - \frac{\dot{\xi}_T\left(n_2^*\right)}{u_1}$$

where $h_B = \dfrac{1}{(N-1)C}$ is the residual headway available up to the moving bottleneck since there remains only $(N-1)$ passing lanes (see Figure 3). This bound is defined as the Legendre-Fenchel transform $H^{\boxtimes}$ of the Hamiltonian $H(\cdot, I_1)$ applied to $\dot{\xi}_T\left(n_2^*\right)$ the spacing imposed by the current moving bottleneck.

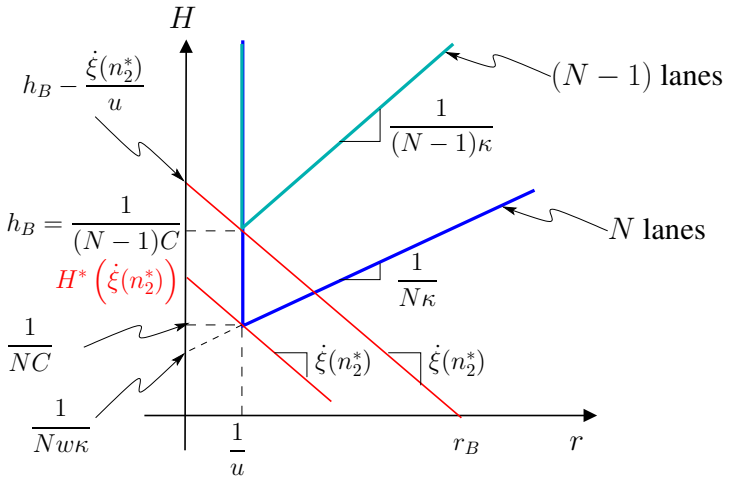

FIGURE 3 Moving bottleneck treatment in Lagrangian-space coordinates for a triangular Hamiltonian or headway-pace FD $H(r)$ defined in (11) with r the pace. (U) and (D) denote respectively the upstream and downstream traffic state with respect to the moving bottleneck position. For the sake of readability, the capacity drop parameter δ is not represented here.

The fourth equation stands for the coupling condition from the point of view of class 2. We assume that if a vehicle of class 2 catches a vehicle of class 1, then it behaves according to a "follow-the-leader" rule. Indeed, class 2 is restricted to the shoulder lane and cannot go on the passing lane(s). Moreover, such a situation may happen if the nearest leader of class 1 is stuck in a congestion and it makes no sense that vehicle of class 2 can overtake. The coupling conditions are thus asymmetric between classes 1 and 2.

Remark 3.1 (Multilanes modeling) *The multilane behaviour of the model (9) is not straightforward at this (continuous) stage. In reality, in the discrete approach, we will use the attribute as a vector in $\mathbb{R}^2$ containing the information about the class of the vehicle and about the lane on which the vehicle is circulating. The lane is updated for each vehicle that can overtake. In a continuous model, it is actually not clear how to express this lane-changing behavior apart from saying that $\dot{I}(n,x) = \varphi(x)$ for a given φ.*

4 Numerical scheme

4.1 Setting of the IBV Problem

Let us introduce the finite steps Δn, $\Delta x > 0$.

Assume that we consider a set of n_{max} vehicles which are divided into k_{max} platoons of Δn vehicles (obviously $n_{max} = n_0 + k_{max}\Delta n$). It is noteworthy that for the sake of clarity, we consider that the label step Δn is the same whatever the vehicle class is. These vehicles are moving on a link $[x_0, x_1]$ divided into l_{max} sections which length is denoted by Δx (obviously $x_1 = x_0 + l_{max}\Delta x$).

We adopt the following notation

$$\begin{cases} n_k := n_0 + k\Delta n, & \text{for any} \quad k \in \{1, \dots, k_{max}\}, \\ x_l := x_0 + l\Delta x, & \text{for any} \quad l \in \{1, \dots, l_{max}\}. \end{cases}$$

Consider the IBV problem (9)-(10) on the computational domain $[n_0, n_{max}] \times [x_0, L]$. Assume that the class-specific Hamiltonians H are triangular, say for any $i \in \{1, 2\}$,

$$H(r, I_i) = \begin{cases} \dfrac{1}{\kappa\, N(I_i)} \left(r + \dfrac{1}{w} \right), & \text{if} \quad r \geq \dfrac{1}{u_i}, \\ +\infty, & \text{otherwise}, \end{cases} \tag{11}$$

where $u_i := u(I_i)$ denotes the free-flow speed of the class i and $N(I_i)$ stands for the number of lanes that are accessible for the class i

$$N(I_i) := \begin{cases} N, & \text{for} \quad i = 1, \\ 1, & \text{for} \quad i = 2. \end{cases}$$

Below, we make precise the definitions of the initial and boundary values $\check{g}_i$, $\hat{g}_i$, G_i for $i \in \{1, 2\}$.

Definition 4.1 (PWA Eulerian upstream boundary condition) *Assume that one can measure the flow values $\{q_{i,k}\}_{k \in [1, k_{max}]}$ for each group of Δn vehicles of class $i \in \{1, 2\}$, at a fixed (and given) location x_0 (thanks to a loop detector for instance).*

We define the piecewise affine (Eulerian) upstream boundary condition for the Hamilton-Jacobi equation (9) as follows

$$T_i(n_K, x_0) = T_i(n_0, x_0) + \sum_{k=1}^{K} h_{i,k}\Delta n, \quad \textit{for any} \quad i \in \{1, 2\}$$

with the headway values

$$h_{i,k} = \frac{1}{q_{i,k}} \quad \textit{for any} \quad k \in [1, k_{max}] \quad \textit{and} \quad i \in \{1, 2\}.$$

We assume moreover that for any $k \in [1, k'_{max}]$ *and* $i \in \{1, 2\}$

$$h_{i,k} = \frac{1}{\Delta n} \int_{n_{k-1}}^{n_k} \check{g}_i(\eta)\, d\eta$$

holds true.

Definition 4.2 (PWA Eulerian downstream boundary condition) *Assume that one can measure the flow values* $\{\hat{q}_{i,k'}\}_{k' \in [1, k'_{max}]}$ *for each group of* Δn *vehicles of class* $i \in \{1, 2\}$*, at a fixed (and given) location* x_1 *(thanks to a loop detector for instance).*

We define the piecewise affine (Eulerian) downstream boundary condition for the Hamilton-Jacobi equation (9) as follows

$$T_i(n_{K'}, x_1) = T_i(n_0, x_1) + \sum_{k=1}^{K'} \hat{h}_{i,k} \Delta n, \quad \textit{for any} \quad i \in \{1, 2\}$$

with the headway values

$$\hat{h}_{i,k} = \frac{1}{\hat{q}_{i,k}}, \quad \textit{for any} \quad k \in [1, k'_{max}] \quad \textit{and} \quad i \in \{1, 2\}\,.$$

We assume moreover that for any $k \in [1, k'_{max}]$ *and* $i \in \{1, 2\}$

$$\hat{h}_{i,k} = \frac{1}{\Delta n} \int_{n_{k-1}}^{n_k} \hat{g}_i(\eta)\, d\eta$$

holds true.

Definition 4.3 (PWA Lagrangian boundary condition) *Assume that one can measure the speed values* $\{v_{i,l}\}_{l \in [1, l_{max}]}$ *for each discrete position distant of* Δx*, for a given leader vehicle* n_0 *of the class* $i \in \{1, 2\}$*.*

We define the piecewise affine (Lagrangian) boundary condition for the Hamilton-Jacobi equation (9) as follows

$$T_i(n_0, x_L) = T_i(n_0, x_0) + \sum_{l=1}^{L} r_{i,l} \Delta x, \quad \textit{for any} \quad i \in \{1, 2\}$$

with the pace values

$$r_{i,l} = \frac{1}{v_{i,l}} \quad \textit{for any} \quad l \in [1, l_{max}] \quad \textit{and} \quad i \in \{1, 2\}\,.$$

We assume moreover that for any $l \in [1, l_{max}]$ *and* $i \in \{1, 2\}$

$$r_{i,l} = \frac{1}{\Delta x} \int_{x_{l-1}}^{x_l} G'_i(\xi)\, d\xi$$

holds true.

4.2 Lax-Hopf formulæ for the MCML model

Representation formulæ for PDEs [24] such as the Lax-Hopf formula for the Hamilton-Jacobi equation [25, 26], enable a fast and exact computation of solutions for the associated PDE.

For instance, Lax-Hopf formula for the LWR model in traffic flow has been used in the Eulerian framework in [27, 28, 29], in the Lagrangian framework in [30] and in the Lagrangian-space framework in [16]. For a synthetic review of these formulæ, the interested reader is referred to [6].

Then for any $(n,x) \in [n_0, n_{max}] \times [x_0, x_1]$, consider the following Lax-Hopf like formulæ (so to speak, here we use a Bellman dynamic programming principle)

$$\begin{aligned} T_1(n,x) = \max \Big\{ & T_1(n, x-\Delta x) + \frac{\Delta x}{u_1}, T_1(n-\Delta n, x+\Delta x) + \frac{\Delta x}{w}, \\ & T_2(n_2^*, x) + \frac{1}{1-\delta} h_B \Big\} \end{aligned} \tag{12}$$

$$\text{with} \quad n_2^* := \text{argmax } T_2(\cdot, x)$$

and

$$\begin{aligned} T_2(n,x) = \max \Big\{ & T_2(n, x-\Delta x) + \frac{\Delta x}{u_2}, \; T_2(n-\Delta n, x+\Delta x) + \frac{\Delta x}{w}, \\ & T_1(n_1^*, x) + H\left(\frac{T_1(n_1^*, x) - T_1(n_1^*, x-\Delta x)}{\Delta x}, I_2 \right) \Big\} \end{aligned} \tag{13}$$

$$\text{with} \quad n_1^* := \text{argmax } T_1(\cdot, x)$$

with the condition

$$\Delta x = \frac{\Delta n}{\kappa}.$$

We recall that $w > 0$ denotes the wave speed, n_i^* is the label of the last vehicle of type $I = I_i$ which has passed through position x and h_B is the residual headway available on the remaining lanes, when crossing the moving bottleneck.

4.3 Some mathematical results

By generalizing the methodology proposed in [17] for the moving bottleneck problem (7) in Eulerian coordinates, one can show that

Proposition 4.4 (Existence of a continuous solution to (9)-(10)) *Assume that $r \mapsto H(r, I_i)$ is convex for any $i \in \{1,2\}$. Then, the IBV problem (9)-(10) admits a solution (T_1, T_2) continuous on $[n_0, +\infty] \times [x_0, x_1]$.*

The proof is out of the scope here. We only assume that this result holds true.

We are now interested in showing the following result:

Proposition 4.5 (Convergence) *Assume that $r \mapsto H(r, I_i)$ is convex for any $i \in \{1, 2\}$. Then the numerical solution $(T_1^\varepsilon, T_2^\varepsilon)$ of the scheme (12) and (13) converges towards a continuous solution (T_1, T_2) of the IBV problem (9)-(10) when $\varepsilon := (\Delta n, \Delta x)$ goes toward zero.*

Proof For the sake of space, we only give the sketch of the proof.

It is worth noticing that the first two terms in the maximum in (12) and (13) are strictly similar to the classical case, say the Lax-Hopf formula (6) for solving the Hamilton-Jacobi equation (3). Indeed, these two terms stand for the usual mesoscopic resolution of the LWR model. The convergence of these two terms is of no concern for us, as the Lax-Hopf formula (6) has already been proved to give an explicit solution to the Hamilton-Jacobi equation (3). The interested reader is referred to [6].

The novelty is the third term that appears in the max in (12) and (13). In each case, we have to ensure that these terms satisfy the coupling conditions between both mesoscopic LWR models. If the coupling conditions are fulfilled, then the *inf-morphism property* (see for instance [27, 16] and references therein) allows us to conclude. Indeed, for each class point of view, the coupling can be seen as an external constraint. The global solution is thus given by the maximum between all the partial solutions obtained for each condition (initial and boundary ones).
The result is straightforward for (13).
For (12), let us fix (n, x) and assume that

$$T_1(n, x) = T_2(n_2^*, x) + \frac{1}{1-\delta} h_B.$$

Moreover, we assume that at a given location x there is no vehicle between the vehicle of class 1 denoted n_1 and its nearest leader of class 2, say n_2^*. This means in particular that

$$T_1(n_1 - \Delta n, x) \leq T_2(n_2^*, x).$$

Thus, we have that for any $s < 0$

$$\begin{aligned}
&H\left(\frac{T_1(n_1, x) - T_1(n_1 - \Delta n, x)}{\Delta n}, I_1\right) - (1-\delta) s \frac{T_1(n_1, x) - T_1(n_1 - \Delta n, x)}{\Delta n} \\
&\geq H\left(\frac{T_1(n_1, x) - T_2(n_2^*, x)}{\Delta n}, I_1\right) - (1-\delta) s \frac{T_1(n_1, x) - T_2(n_2^*, x)}{\Delta n} \\
&\geq h_B - (1-\delta)\frac{s}{u_1} \\
&\geq \frac{N-1}{N} h_B - (1-\delta)\frac{s}{u_1} \\
&\geq H^{\boxtimes}\left((1-\delta)s, I_1\right).
\end{aligned}$$

Taking the limit Δn going to zero and setting $s = \dot{\xi}(n_2^*)$, we get the result. This ends the proof. □

5 Numerical examples

5.1 Impact of a single "slow vehicle"

The numerical scheme (12)-(13) has been applied to a link composed of two lanes located immediately upstream a diverge (at $x = x_1$) with two output branches. The incoming link length is set to $L = x_1 - x_0 = 1000m$. The demand at $x = x_0$ is set to $q = 1\ vps$ (vehicle per second) for class 1. A single vehicle from class 2 drives through the link with a maximum speed $u_2 = 10m/s$, while vehicles from class 1 have a maximum speed $u_1 = 25m/s$. The congested parameters are set to $w = 5m/s$ and $k_x = 0.14veh/m$ for both classes. The simulation duration is set to $200s$ with $\delta = 0$.

In the remaining of the section, "fast vehicles" (resp. "slow vehicles") designate vehicles from class 1 (resp. 2).

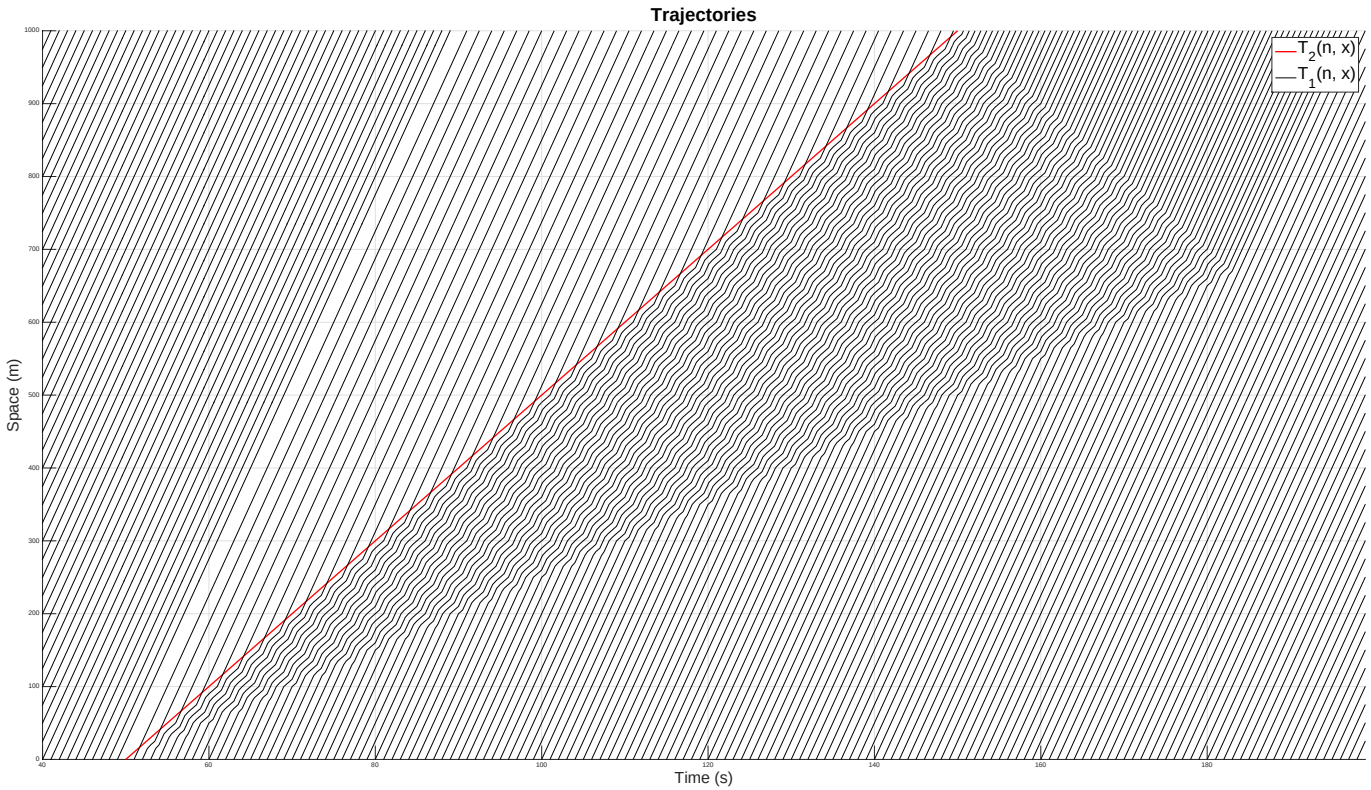

FIGURE 4 Impact of single slow vehicle (class 2) on fast vehicles (class 1)

Figure 4 depicts $T(n,x)$ in the time-space plan, for vehicle from class 1 (black lines) and class 2 (red line). The consistency of the result with the well-established moving bottleneck theory is verified. The flow upstream the slow vehicle exceeds the maximum flow that can overtake. The MB is said to be active and separates two traffic states: (i) a free flow state downstream the MB with $h = h_B$ and (ii) a congested state upstream the MB.

Here it has been assumed that no capacity drop occurs, $\delta = 0$. Then four levels of capacity drop have been tested: $\delta = \{0.2, 0.4, 0.6, 1\}$. The results are presented in Figure 5.

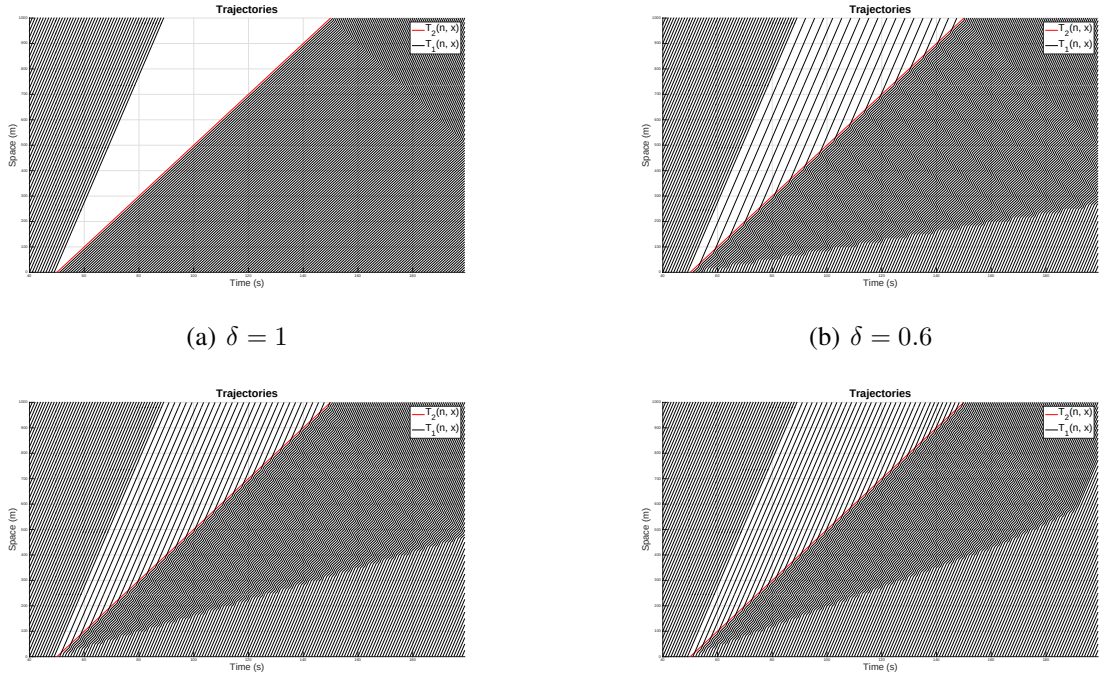

(a) $\delta = 1$ (b) $\delta = 0.6$

(c) $\delta = 0.4$ (d) $\delta = 0.2$

FIGURE 5 Impact of δ on traffic states surrounding an active MB

Obviously the slow vehicle surrounding conditions highly depend on the capacity drop parameters, which drives the maximum flow that overtakes. Comparing Figures 5(a), 5(b), 5(c) and 5(d), it is worth noticing that δ can also be interpreted as a parameter that relaxes the FIFO rule. When $\delta = 1$, fast vehicles cannot overtake slow vehicles and the traffic flow is FIFO. Vehicle upstream the diverge share the same delay independent of the destination (class). When $\delta \neq 0$, the FIFO rule is relaxed and vehicles from "fast class" are more and more inclined to overtake vehicles from "slow class".

5.2 Simulation with a mixed traffic

Finally, an advanced simulation scenario has been implemented with the same link characteristics, where the vehicle classes have the same characteristics as above. The demand at $x = x_0$ is set to $q = 1\ vps$ with the following distribution per class: class 1 = 95% and class 2 = 5%. The simulation results are illustrated in Figure 6.

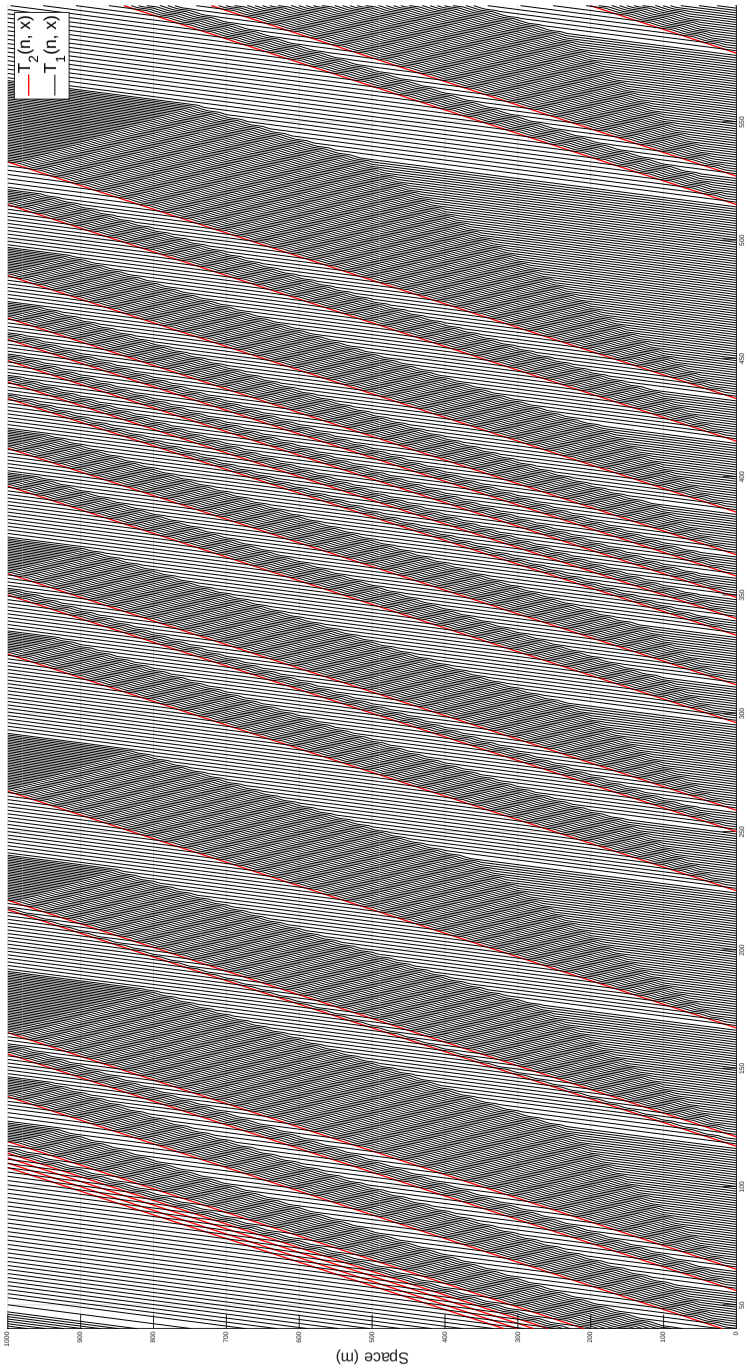

FIGURE 6 Simulation results

Here again, slow vehicles act as active moving bottlenecks. The flow downstream slow vehicles is bounded and fast vehicles accumulate behind.

FIGURE 7 Simulation results

It can also be seen from figure 7 that travel times experienced by fast vehicles oscillate around $60s$. This mean travel time is a trade-off between $40s$ (when no interaction occurs between classes) and $100s$ (when class 1 and 2 strictly respect the FIFO rule). It is directly related to the simulation parameters, and first of all δ which drives the level of relaxation of the FIFO rule. We conclude from this scenario that the proposed multiclass model:

- provides a more realistic framework to simulate traffic condition upstream diverge. It allows for relaxing the FIFO rule while considering the interactions between vehicle classes.
- the calibration of δ is of paramount importance for practical application. Further research is needed to propose accurate methodology to calibrate δ accurately and to identify factors that impact δ (lane ratio, class distribution, speed difference, etc.).

6 Conclusion and perspectives

We have introduced a new event-based mesoscopic model for multi-class traffic flow modeling on multi-lane sections. The basis model was first introduced by Leclercq and Bécarie [5] and deals with traffic flow on mono-pipe links, even if it can take into account simple junction models and two-flows representation thanks to the theory of moving bottlenecks. The model has been proven

to be very attractive to simulate traffic flow on wide networks since it only keeps track of individual passing times at the boundaries of the network.

Among the perspectives, we would be interested in dealing with real traffic data to validate the continuous model, even if we are aware that these data need to be precise enough such that one can make the distinction between vehicle classes for example cars and trucks. A step further would be data assimilation for real-time applications such as traffic state estimation and forecast. We are also looking forward coupling our approach with lane flow distribution as proposed for instance in [*31*] where the authors proposed a mechanism to show how variable speed limits help to delay the congestion onset.

In a quite different fashion, another extension of this work would be to consider the mesoscopic formulation of the GSOM family (as discussed in Section 3.1) and to assume that the moving bottlenecks are (known) internal boundary conditions. A numerical solution could be obtained by extending the algorithm described in [*32*], when assuming a triangular fundamental diagram $H(\cdot, I)$.

7 Acknowledgements

The authors are sincerely grateful to Prof. Ludovic Leclercq for fruitful discussions during the preparation of this paper and to the three anonymous referees whose comments helped to improve the presentation of this work.

REFERENCES

[1] Lighthill, M. J. and G. B. Whitham. On kinematic waves II. A theory of traffic flow on long crowded roads. *Proceedings of the Royal Society of London. Series A. Mathematical and Physical Sciences*, Vol. 229, No. 1178, The Royal Society, 1955, pp. 317–345.

[2] Richards, P. I. Shock waves on the highway. *Operations research*, Vol. 4, No. 1, INFORMS, 1956, pp. 42–51.

[3] Bellomo, N. and C. Dogbe. On the modeling of traffic and crowds: A survey of models, speculations, and perspectives. *SIAM review*, Vol. 53, No. 3, SIAM, 2011, pp. 409–463.

[4] Newell, G. F. A simplified car-following theory: a lower order model. *Transportation Research Part B: Methodological*, Vol. 36, No. 3, Elsevier, 2002, pp. 195–205.

[5] Leclercq, L. and C. Bécarie, A meso LWR model designed for network applications. In *Transportation Research Board 91th Annual Meeting*, 2012, Vol. 118, p. 238.

[6] Laval, J. A. and L. Leclercq. The Hamilton–Jacobi partial differential equation and the three representations of traffic flow. *Transportation Research Part B: Methodological*, Vol. 52, Elsevier, 2013, pp. 17–30.

[7] Hoogendoorn, S. P. and P. H. Bovy. Continuum modeling of multiclass traffic flow. *Transportation Research Part B: Methodological*, Vol. 34, No. 2, Elsevier, 2000, pp. 123–146.

[8] Wong, G. and S. Wong. A multi-class traffic flow model–an extension of LWR model with heterogeneous drivers. *Transportation Research Part A: Policy and Practice*, Vol. 36, No. 9, Elsevier, 2002, pp. 827–841.

[9] van Wageningen-Kessels, F., *Multi-class continuum traffic flow models: Analysis and simulation methods*. Ph.D. thesis, Ph. D. thesis, Delft University of Technology/TRAIL Research School, Delft, The Netherlands, 2013.

[10] van Wageningen-Kessels, F., H. van Lint, K. Vuik, and S. Hoogendoorn. Genealogy of traffic flow models. *EURO Journal on Transportation and Logistics*, Springer, 2014, pp. 1–29.

[11] Daganzo, C. F. A behavioral theory of multi-lane traffic flow. Part I: Long homogeneous freeway sections. *Transportation Research Part B: Methodological*, Vol. 36, No. 2, Elsevier, 2002, pp. 131–158.

[12] Gazis, D. C. and R. Herman. The moving and phantom bottlenecks. *Transportation Science*, Vol. 26, No. 3, INFORMS, 1992, pp. 223–229.

[13] Newell, G. F. A moving bottleneck. *Transportation Research Part B: Methodological*, Vol. 32, No. 8, Elsevier, 1998, pp. 531–537.

[14] Munoz, J. C. and C. Daganzo. Experimental characterization of multi-lane freeway traffic upstream of an off-ramp bottleneck. *California Partners for Advanced Transit and Highways (PATH)*, 2000.

[15] Munoz, J. C. and C. F. Daganzo. The bottleneck mechanism of a freeway diverge. *Transportation Research Part A: Policy and Practice*, Vol. 36, No. 6, Elsevier, 2002, pp. 483–505.

[16] Jin, P. J., K. Han, and B. Ran, Some Theoretical and Practical Perspectives of the Travel Time Kinematic Wave Model: Generalized Solution, Applications, and Limitations. In *Transportation Research Board 93rd Annual Meeting*, 2014, 14-5514.

[17] Delle Monache, M. L. and P. Goatin. Scalar conservation laws with moving constraints arising in traffic flow modeling: an existence result. *Journal of Differential equations*, Vol. 257, No. 11, Elsevier, 2014, pp. 4015–4029.

[18] Lebacque, J.-P., S. Mammar, and H. H. Salem, Generic second order traffic flow modelling. In *Transportation and Traffic Theory 2007. Papers Selected for Presentation at ISTTT17*, 2007.

[19] Laval, J. A. A macroscopic theory of two-lane rural roads. *Transportation Research Part B: Methodological*, Vol. 40, No. 10, Elsevier, 2006, pp. 937–944.

[20] Daganzo, C. F. The cell transmission model, part II: network traffic. *Transportation Research Part B: Methodological*, Vol. 29, No. 2, Elsevier, 1995, pp. 79–93.

[21] Newell, G. F. A simplified theory of kinematic waves in highway traffic, part I–III. *Transportation Research Part B: Methodological*, Vol. 27, No. 4, Elsevier, 1993, pp. 281–313.

[22] Lebacque, J.-P., The Godunov scheme and what it means for first order traffic flow models. In *Internaional symposium on transportation and traffic theory*, 1996, pp. 647–677.

[23] Ni, D. and J. D. Leonard II. A simplified kinematic wave model at a merge bottleneck. *Applied Mathematical Modelling*, Vol. 29, No. 11, Elsevier, 2005, pp. 1054–1072.

[24] Evans, L. C. *Partial differential equations (graduate studies in mathematics, vol. 19)*. American Mathematics Society, 2009.

[25] Hopf, E. Generalized solutions of non-linear equations of first order. *Journal of Mathematics and Mechanics*, Vol. 14, 1965, pp. 951–973.

[26] Lax, P. D. Hyperbolic systems of conservation laws II. *Communications on Pure and Applied Mathematics*, Vol. 10, No. 4, Wiley Online Library, 1957, pp. 537–566.

[27] Claudel, C. G. and A. M. Bayen. Lax–Hopf based incorporation of internal boundary conditions into Hamilton–Jacobi equation. Part i: Theory. *Automatic Control, IEEE Transactions on*, Vol. 55, No. 5, IEEE, 2010, pp. 1142–1157.

[28] Claudel, C. G. and A. M. Bayen. Lax–Hopf based incorporation of internal boundary conditions into Hamilton–Jacobi equation. Part ii: Computational methods. *Automatic Control, IEEE Transactions on*, Vol. 55, No. 5, IEEE, 2010, pp. 1158–1174.

[29] Mazaré, P.-E., A. H. Dehwah, C. G. Claudel, and A. M. Bayen. Analytical and grid-free solutions to the Lighthill–Whitham–Richards traffic flow model. *Transportation Research Part B: Methodological*, Vol. 45, No. 10, Elsevier, 2011, pp. 1727–1748.

[30] Han, K., T. Yao, and T. L. Friesz. Lagrangian-based hydrodynamic model: Freeway traffic estimation. *arXiv preprint arXiv:1211.4619*, 2012.

[31] Duret, A., S. Ahn, and C. Buisson. Lane flow distribution on a three-lane freeway: General features and the effects of traffic controls. *Transportation research part C: emerging technologies*, Vol. 24, Elsevier, 2012, pp. 157–167.

[32] Costeseque, G. and J.-P. Lebacque. A variational formulation for higher order macroscopic traffic flow models: numerical investigation. *Transportation Research Part B: Methodological*, Vol. 70, Elsevier, 2014, pp. 112–133.